Appl. Sci. Converg. Technol. 30 (3); 78-80 (2021)
https://doi.org/10.5757/ASCT.2021.30.3.78

eISSN: 2288-6559

Research Paper

Current Tunneling Characterization of Oxidized Black Phosphorus by Graphite Thin Film Electrodes

Received 6 May, 2021; revised 20 May, 2021; accepted 24 May, 2021

Jong Yun Kim[a], Oh Hun Gwon[b], Seok-Ju Kang[a], Hye Ryung Byun[a], and Young-Jun Yu[a,b,*]

[a]Institute of Quantum Systems, Chungnam National University, Daejeon 34134, Republic of Korea
[b]Department of Physics, Chungnam National University, Daejeon 34134, Republic of Korea

*Corresponding author E-mail: yjyu@cnu.ac.kr

ABSTRACT

In this work, oxidized black phosphorus (BP) was trapped in the top and bottom interfaces of graphite thin film electrodes by hexagonal boron nitride (hBN) encapsulation. Upon using partial encapsulation of hBN on BP, the oxidation of bare BP area led to the oxidation of hBN encapsulated whole BP, and this oxidized BP could be confined in the hBN layer. Furthermore, by attaching graphite thin film electrodes on and underneath the oxidized BP layer, charge carrier injection and extraction behavior from measuring the current tunneling was characterized by applying a bias voltage between the top and the bottom graphite thin film electrodes. The electrical characteristics according to applied bias voltage was confirmed with a double log plot. It was found that the ohmic current region exists in the low voltage state, and the space-charge-limited conduction region exists in the high voltage state.

Keywords: Black phosphorus, Hexagonal boron nitride, Graphite thin film, Oxidation

1. Introduction

Black phosphorus (BP), with its high charge carrier mobility (> ~ 200 cm^2/Vs) and resulting bandgap (0.3–2.0 eV), has been favored in atomically thin and high-speed semiconductor devices [1–8]. However, there are certain challenges with applying BP in optical and electrical devices, with the instability (i.e., oxidation) of BP in air being a critical one. Since the oxidation period of BP in air in both single- and multi-layers is reported to be from 1 hour to 2 weeks, oxidation on a thick BP surface and the disappearance of thin BP can be easily observed by optical microscopy [9–12]. Because of the instability of BP in air, various methods to protect BP from oxygen have been proposed. Although hexagonal boron nitride (hBN) has been widely researched regarding its protective capability of BP [13, 14], BP without full hBN encapsulation still leads to oxidation, which is initiated in the area exposed to air. It is difficult to avoid BP oxidation completely. However, if we change our point of view oppositively, an artificial oxidized layer is able to be generated in the interface between two-dimensional layers. In this work, upon preparing partially encapsulated BP by hBN, an oxidized BP layer under hBN by initially oxidizing from bare BP was created. The current tunneling characterization of this oxidized BP layer was investigated by using graphene-electrodes sandwiched heterostructures. Because oxides can be applied to memory devices [15–19], the electrical characterization of an oxidized BP layer will make a good reference for atomically thin memory device applications.

2. Experimental details

In order to study the current transport behavior of oxidized BP, we employed graphite thin film electrodes, as shown in Fig. 1. The bottom graphite thin film (BG) on 280-nm-thick SiO_2 substrate was mechanically exfoliated [Fig. 1(a)] and the BP flake was transferred to the BG [Fig. 1(b)]. The top graphite thin film (TG) was stacked on the BP/BG/SiO_2 area [Fig. 1(c)] for measuring the current tunneling behavior; this TG/BP/BG/SiO_2 heterostructure was encapsulated by hBN, as shown in Fig. 1(d). This two-dimensional material stacking process was performed using a micro-transferring system with polydimethylsiloxane (PDMS) stamping [14, 19, 20]. The TG and the BG were then contacted using Cr/Au (10 nm / 100 nm) electrodes via normal e-beam lithography [see Fig. 1(e)]. Upon employing a semiconductor parameter analyzer (Keithley 4200), the charge carrier transport behavior of oxidized BP between the TG and the BG was characterized, as shown in Fig. 1(e).

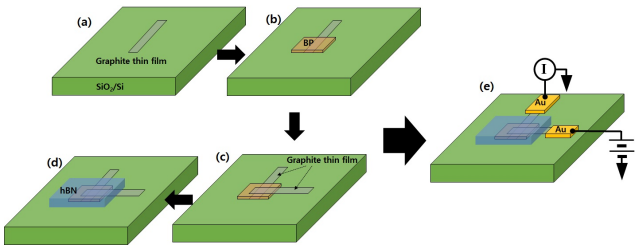

Figure 1. Schematic diagram of hBN/TG/BP/BG heterostructure fabrication. (a) Mechanical exfoliation of BG on SiO_2/Si substrate. (b) Transfer of BP to BG/SiO_2/Si substrate. (c) Transfer of TG to BP/BG/SiO_2/Si heterostructure. (d) Encapsulation of hBN on TG/BP/BG/SiO_2/Si heterostructure. (e) Cr/Au electrodes contact with TG and BG and electrical characterization.

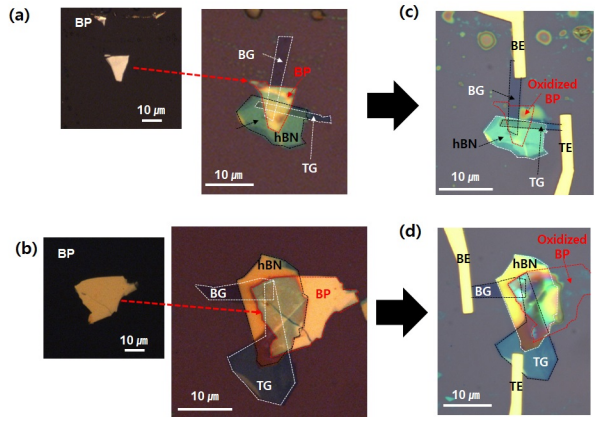

Figure 2. (a) Optical image of (left) BP layer (~ 40 nm thickness) on PDMS transferring polymer layer, and (right) hBN/TG/BP/BG/SiO_2/Si heterostructure with ~ 10 nm thick hBN. (b) Optical image of (left) BP layer (~ 60 nm thickness) on PDMS transferring polymer layer, and (right) hBN/TG/BP/BG/SiO_2/Si heterostructure with ~ 90 nm thick hBN. Thicknesses of TG and BG are around 10 and 5 nm, respectively. (c) Optical image of hBN/TG/BP/BG/SiO_2/Si heterostructure (~ 10-nm-thick hBN and ~ 40-nm-thick BP) after contact with Au top-electrode (TE) and bottom-electrode (BE) on TG and BG, respectively. (d) Optical image of hBN/TG/BP/BG/SiO_2/Si heterostructure (~ 90-nm-thick hBN and ~ 60-nm-thick BP) after contact with Au TE and BE on TG and BG, respectively. The oxidized BP disappears due to exposure to air during the Au electrode contact fabrication process.

3. Results and discussion

Figure 2 shows the hBN/TG/BP/BG heterostructure with a thickness of ~ 5 and ~ 10 nm for the BG and TG, respectively. The hBN and BP had different thicknesses: thin hBN (~ 10 nm), BP (~ 40 nm) for Fig. 2(a); and thick hBN (~ 90 nm), BP (~ 60 nm) for Fig. 2(b). While the BP layers in Figs. 2(a) and 2(b) can be clearly observed by optical microscopy when the process of stacking was just completed for the hBN/TG/BP/BG heterostructures, the disappearing BP layers in the heterostructures appeared during the Au electrode contact fabrication process [see Figs. 2(c) and 2(d)]. This behavior is well known

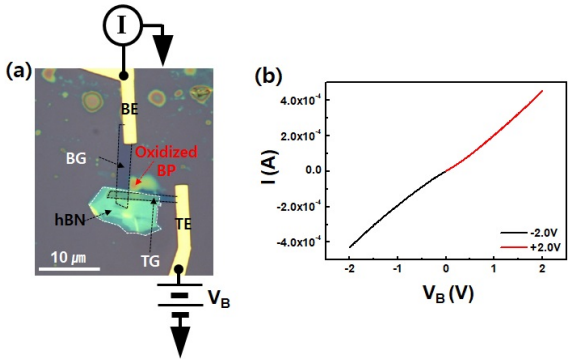

Figure 3. (a) Optical image of hBN/TG/BP/BG/SiO_2/Si heterostructure (~ 10-nm-thick hBN and ~ 40-nm-thick BP) after contact with Au electrodes on TG and BG. Schematic diagram of tunneling current from applying a bias voltage between TG and BG electrodes. (b) Current (I) as a function of bias voltage (V_B) between TG (TE) and BG (BE) electrodes. The red and black lines represent forward (+) and backward (-) sweep.

as the oxidation of BP in air [9–12]. A period of ~ 1 week was given for the Au electrode contact fabrication on the TG and BG. This was a sufficient length of time to see the BP layer disappear due to oxidation in air.

According to this phenomenon, thin BP (~ 40 nm) encapsulated by thin hBN (~ 10 nm) in hBN/TG/BP/BG heterostructures exhibits an almost linear current curve (I) as a function of the bias voltage (V_B) between TG and BG, as shown in Fig. 3. As confirmation of the oxidized BP in the hBN/TG/BP/BG heterostructures in Fig. 3(a), we did not observe even oxidized BP layer in overlapped by TG and BG area. The I-V_B curve for the hBN/TG/BP/BG heterostructure exhibited a tunnel resistance of ~ 5 kΩ, and this value could be corresponded to only contact resistance between TG and BG electrodes without a tunnel barrier [21].

Meanwhile, for thick BP (~ 60 nm) encapsulated by thick hBN (~ 90 nm) in the hBN/TG/BP/BG heterostructure, slightly bright areas [marked by the red dashed boxes and arrows in Fig. 4(a)] were observed in the overlapping TG and BG area. The hysteresis of the cur-

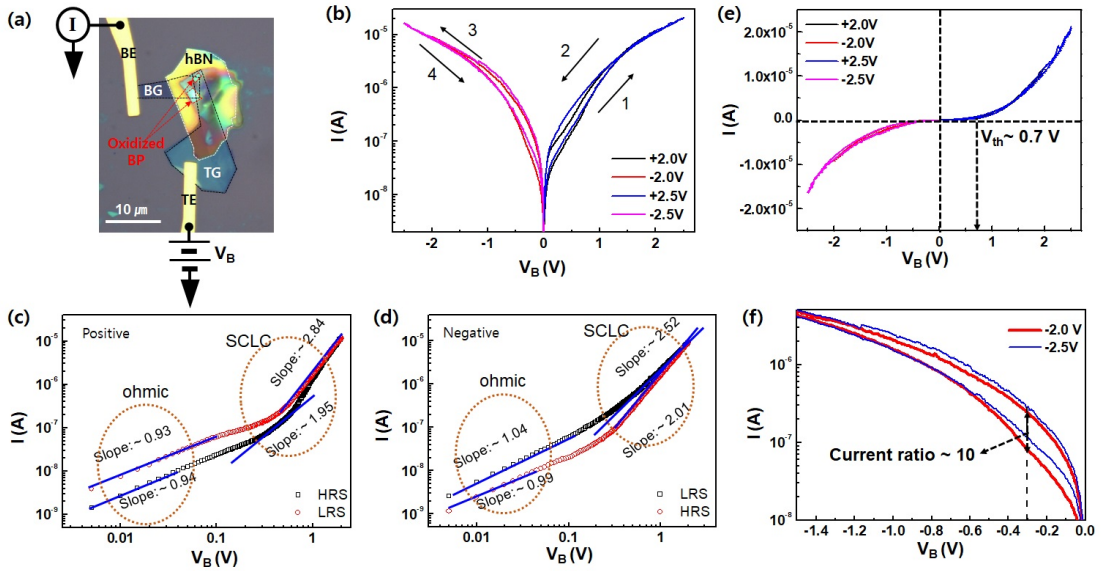

Figure 4. (a) Optical image of hBN/TG/BP/BG/SiO_2/Si heterostructure (~ 90-nm-thick hBN and ~ 60-nm-thick BP) after contact with Au electrodes on TG and BG. Schematic diagram of tunneling current from applying bias voltage between TG and BG electrodes. (b) Current (I) as a function of bias voltage (V_B) between TG (TE) and BG (BE) electrodes. The double logarithmic scale plots of (c) positive and (d) negative voltage sweep region for (b) I-V_B curve. (e) Linear scale (I) as a function of V_B between TG (TE) and BG (BE) electrodes. (f) Enlarged I-V_B curve of (b). The red and blue lines represent -2.0 and -2.5 V dual sweep, respectively.

rent curve could be seen for the forward and backward sweep of V_B [marked by arrows and numbers 1–4 in Fig. 4(b)]. By employing a logarithmic scale of both I and V_B values for positive and negative voltage sweep regions, as shown in Figs. 4(c) and 4(d), respectively, the ohmic and space-charge-limited conductance regions with I-V_B curve slops as ~ 1 and ~ 2, respectively, could be characterized [22–24]. This indicates that the potential barrier of oxidized BP resulting in ohmic behavior under low V_B ~ 0.1 V is suppressed by charge carrier injection on oxidized BP, leading to space-charge-limited conductance behavior for positive and negative V_B sweep larger than ± 0.1 V, respectively. As a result, the I-V_B exhibited a general tunneling behavior with a threshold voltage (V_{th}) of ~ ± 0.6 V, as shown in Fig. 4(e). This indicates that there is oxidized BP between the TG and the BG electrodes, and the storing and releasing charge carrier on oxidized BP between TG and BG for the forward and backward sweep of V_B gave rise to a current ratio of 10 for the hysteresis area at V_B = -0.3 V, as shown in Fig. 4(f). Thus, we confirmed that the oxidized BP was confined in the heterojunction with thick hBN (≥ 90 nm) encapsulation. As a result, although the current ratio of ~ 10 was not particularly large, it nonetheless suggested the potential for oxidized BP layer utilization for memory application.

4. Conclusions

In this work, an oxidized black phosphorus (BP) layer in the interface between graphite thin film electrodes with hexagonal boron nitride (hBN) encapsulation was examined. For thick hBN (> 90 nm) encapsulation, the oxidized BP layer can be locked in the hBN layer, with the charge carrier storing or releasing on this oxide layer with a forward (+) and backward (-) sweep of a bias voltage between the top and bottom graphite thin film electrodes. Although the current ratio and memory window is not especially large, the potential for oxidized BP layer application in memory devices remains meaningful.

Acknowledgements

This work was supported by the research fund of Chungnam National University.

References

[1] L. Li, Y. Yu, G. Ye, Q. Ge, X. Ou, H. Wu, D. Feng, X. Chen, and Y. Zhang, Nat. Nanotechnol. 9, 372 (2014).
[2] D. K. Kim, S. B. Hong, K. Jeong, C. Lee, H. Kim, and M. H. Cho, ACS Nano 13, 1683 (2019).
[3] D. Lee, Y. Choi, E. Hwang, M. S. Kang, S. Lee, and J. H. Cho, Nanoscale 8, 9107 (2016).
[4] J. Liu, Y. Chen, Y. Li, H. Zhang, S. Zheng, and S. Xu, Photonics Res. 6, 198 (2018).
[5] T. Chen, P. Zhao, X. Guo, and S. Zhang, Nano Lett. 17, 2299 (2017).
[6] M. Zhu, S. Kim, L. Mao, M. Fujitsuka, J. Zhang, X. Wang, and T. Majima, J. Am. Chem. Soc. 139, 13234 (2017).
[7] S. Yan, B. Wang, Z. Wang, D. Hu, X. Xu, J. Wang, and Y. Shi, Biosens. Bioelectron. 80, 34 (2016).
[8] J. Zhou, Z. Li, M. Ying, M. Liu, X. Wang, X. Wang, L. Cao, H. Zhang, and G. Xu, Nanoscale 10, 5060 (2018).
[9] Y. Huang *et al.*, Preprint at https://arxiv.org/ftp/arxiv/papers/1511/1511.09201.pdf (2015).
[10] J. S. Kim, Y. Liu, W. Zhu, S. Kim, D. Wu, L. Tao, A. Dodabalapur, K. Lai, and D. Akinwande, Sci. Rep. 5, 8989 (2015).
[11] B. Yang *et al.*, Adv. Mater. 28, 9408 (2016).
[12] J. Kim, S. K. Baek, K. S. Kim, Y. J. Chang, and E. J. Choi, Curr. Appl. Phys. 16, 165 (2016).
[13] R. A. Doganov *et al.*, Nat. Commun. 6, 6647 (2015).
[14] Z. H. Wang, A. Islam, R. Yang, X. Q. Zheng, and P. X. L. Feng, J. Vac. Sci. Technol. B 33, 052202 (2015).
[15] M. H. Jeong, D. H. Kwak, H. S. Ra, A. Y. Lee, and J. S. Lee, ACS Appl. Mater. Interfaces 10, 19069 (2018).
[16] D. Kumar, R. Aluguri, U. Chand, and T. Y. Tseng, Ceram. Int. 43, S547 (2017).
[17] Y. Yang, S. Choi, and W. Liu Nano Lett. 13, 2908 (2013).
[18] M. Chen, H. Nam, S. Mi, G. Priessnitz, I. M. Gunawan, and X. Liang, ACS Nano 8, 4023 (2014).
[19] H. Shen, J. Ren, J. Li, Y. Chen, S. Lan, J. Wang, H. Wang, and D. Li, ACS Appl. Mater. Inter. 12, 58428 (2020).
[20] C. Hou, L. Yang, B. Li, Q. Zhang, Y. Li, Q. Yue, Y. Wang, Z. Yang, and L. Dong, Sensors 18, 1668 (2018).
[21] G. H. Lee, Y. J. Yu, C. Lee, C. Dean, K. L. Shepard, P. Kim, and J. Hone, Appl. Phys. Lett. 99, 243114 (2011).
[22] H. Y. Jeong *et al.*, Nano Lett. 10, 4381 (2010).
[23] A. Rose, Phys. Rev. 97, 1538 (1955).
[24] R. Dong *et al.*, Appl. Phys. Lett. 90, 042107 (2007).